INTERNATIONAL JOURNAL OF ENERGY RESEARCH
Int. J. Energy Res. 2000; **24**:665–678

Effects of shingle absorptivity, radiant barrier emissivity, attic ventilation flowrate, and roof slope on the performance of radiant barriers

Mario A. Medina*

Architectural Engineering Department, The University of Kansas, Lawrence, KS 66045-2222, U.S.A.

SUMMARY

This paper presents a parametric study of the effects that shingle absorptivity, radiant barrier emissivity, attic ventilation flowrate, and roof slope have on the performance of radiant barriers in symmetrical residential attics. A heat balance model was developed to investigate these effects. The model was validated against experimental data and was found to predict with good accuracy. Of the four parameters investigated, only emissivity of the radiant barriers had first-order effects on their performance. Variations in the performance of the horizontal radiant barrier (HRB) configuration were minimal in the other three parameters. The truss radiant barrier (TRB) configuration showed slightly more variations because of the presence of uncovered end-gables. This paper presents a brief description of the heat balance model, the parametric studies and conclusions. Copyright © 2000 John Wiley & Sons, Ltd.

KEY WORDS: radiant barriers; attic ventilation; building heat and mass transfer modelling

INTRODUCTION

In the United States, one of the major ends uses of energy is space conditioning in residential and commercial buildings. Buildings consume approximately 36 per cent of the total energy used in the country. The estimated consumption of energy in the residential and commercial sectors in 1997 was estimated at 9.88×10^9 MWh, up 15 per cent from 1990 estimates (EIA, 1998). Predicted growth in housing will significantly increase energy demands. The need for space cooling during the summer represents the major source of energy use in the residential sector.

As a direct consequence of increased pressure for reducing energy use in residences, building insulation systems have been the topic of a substantial amount of research in the past decades. Most new houses are built with walls and attics insulated by lightweight fibrous insulation. The amount of insulation that can be added to a wall or to an attic space is mostly determined by the physical constraints of the frames of the structures. Most wall frames will allow between 5 and

*Correspondence to: Mario A. Medina, Architectural Engineering Department, The University of Kansas, Lawrence, KS 66045-2222, U.S.A.

Received 19 July 1999
Accepted 3 September 1999

16 cm (2–6 in) of insulation to be placed in the walls and most attics will allow anywhere between 5 and 25 cm (2–9.5 in) of insulation to be placed in the ceiling frame before the extra insulation obstructs the attic ventilation air and/or creates an excessive weight on the ceiling structure. Any significant improvement made towards increasing the resistance value of the insulation can reduce the amount of insulation required while still producing significant reductions in both space cooling and heating loads. Radiant barrier systems offer an alternative way of increasing the heat flow resistance in attics of residences without increasing the bulk size of the insulation.

Radiant barriers are thin metal sheets, usually aluminium, characterized by having at least one low emissivity surface of less than 0.05. Radiant barriers have received increased attention because of their potential to reduce the radiant heat absorbed through the ceiling in a residence. At summer peak times, no less than 40 per cent of the energy that enters the conditioned space through the ceiling is the direct result of radiant energy from the attic deck. Because of its low emissivity, a radiant barrier placed facing the attic air space can prevent as much as 95 per cent of the attic deck infrared radiation from being transferred to the top of the insulation. This radiation blockage reduces the amount of energy gained by the conditioned space through the ceiling. For retrofit cases, two radiant barrier installation configuration have received the most consideration, the horizontal radiant barrier (HRB) and the truss radiant barrier (TRB) configurations. The HRB installation places the radiant barrier flat over the ceiling frame, while the TRB installation places the radiant barrier against the rafters of the attic. Under the TRB configuration, a new air space is formed between the barrier and the attic deck.

Engineering models are needed to understand better the physical phenomena affecting the performance of radiant barriers. The heat balance (HB) method (ASHRAE, 1997) is an approach that allows hourly thermal-load calculation to be performed based on the physical description of the building, the hour's ambient weather conditions, and a history of previous temperatures and heat fluxes. The HB method is based on an instantaneous heat balance equation in which, for each space simulated, all the relevant heat fluxes are considered. This approach was used in this study to model the attic space of a residential building.

Several of the parameters expected to affect radiant barrier performance were studied. These included roof absorptivity, radiant barrier emissivity, attic ventilation flowrate, and roof slope. The parametric studies included both cooling and heating seasons. The cooling season included the months of June–August. The heating season included the months of December–February. The parameters' effects on radiant barriers' performance are presented in terms of seasonal ceiling heat flow reductions (SCHFR), defined as the percent difference over a season between the ceiling heat flow in the control house and that in the retrofit house. The weather tapes used to drive these simulations were from Austin, TX. An insulation level of 3.35 $m^2 K W^{-1}$ (R-19) was used and kept constant. Also, an attic ventilation rate of 5.1 $l s^{-1} m^{-2}$ of attic floor (1 CFM ft^{-2} of attic floor) was used, and kept constant, except for the case in which attic airflow rate was the parameter being studied.

DESCRIPTION OF THE MODEL

The model followed the methodology described by Pedersen *et al.* (1998). These required that heat balances be set-up for outside and inside surfaces and for the air zone and that these be coupled to the wall conduction process. Once these processes were described they were solved

simultaneously using an iterative solution. The attic model is described in detail in Medina *et al.* (1998a). A brief description follows.

The attic used in the development of the model was a five-sided symmetrical attic composed of two pitched roof sections, two vertical gable-end sections, and one horizontal ceiling frame. For any surface, the heat balance equation was

$$Q_{\text{conducted (to/from)}} + \text{Heat Stored} + Q_{\text{convected (to/from)}} + Q_{\text{radiated (net)}} + Q_{\text{latent (cond/evap)}} = 0 \quad (1)$$

Using conduction transfer function notation, for an attic exterior surface, Equation (1) is expressed as (on a rate basis)

$$\sum_{j=0,i=1}^{N,S} Y_{i,j}(T\text{si}_{i,n\Delta-j} - T_r) - \sum_{j=0,i=1}^{N,S} X_{i,j}(T\text{so}_{i,n\Delta-j} - T_r) + \text{CR}_i q''_{o(i,n\Delta-1)} + \text{ho}_i(T_{\text{amb}} - T\text{so}_{i,n\Delta})$$

$$+ \text{hro}_i(T_{\text{sky/surr}} - T\text{so}_{i,n\Delta}) + \alpha q''_{\text{sol},i} = 0 \quad (2)$$

and for an attic interior surface as

$$\sum_{j=0,i=1}^{N,S} Z_{i,j}(T\text{si}_{i,n\Delta-j} - T_r) - \sum_{j=0,i=1}^{N,S} Y_{i,j}(T\text{so}_{i,n\Delta-j} - T_r) + \text{CR}_i q''_{i(i,n\Delta-1)} + \text{hi}_i(T\text{si}_{i,n\Delta} - T_{\text{attic air},n\Delta})$$

$$+ \sum_{k=1,i=1}^{s,s} \text{hri}_{i,k}(T\text{si}_{i,n\Delta} - T\text{si}_{k,n\Delta}) + q''_{\text{latent},i} = 0 \quad (3)$$

The convection coefficients ho_i and hi_i were estimated using published correlations based on Nusselt numbers (ASHRAE, 1998). In equation form,

$$\bar{h} = \frac{\overline{\text{Nu}}\, k}{L} \quad (4)$$

This approach combined the natural and forced convection Nusselt numbers (Churchill, 1977; Chen *et al.*, 1986) using

$$\overline{\text{Nu}}^n = \overline{\text{Nu}}_F^n \pm \overline{\text{Nu}}_N^n \quad (5)$$

Also, different expressions of Nusselt number were formulated depending on heat flow direction and surface orientation. The indoor radiation coefficients were estimated by

$$\text{hri}_{i,k} = G_{i,k}\sigma(T_i^2 + T_k^2)(T_i + T_k) \quad (6)$$

where

$$G_{i,j} = \frac{\varepsilon_i}{1 - \varepsilon_i}\psi_{i,k} \quad (7)$$

and where previous values of temperatures were used. For the net radiation on outer attic surfaces to the sky and surroundings, the coefficient was formulated as

$$\mathrm{hro_i} = \varepsilon_{\mathrm{i,out}}\sigma(T_{\mathrm{i,out}}^2 + T_{\mathrm{sky/surr}}^2)(T_{\mathrm{i,out}} + T_{\mathrm{sky/surr}}) \tag{8}$$

The total solar radiation incident on an inclined surface was estimated by

$$q''_{\mathrm{sol}} = I_{\mathrm{d}} + R_{\mathrm{b}} I_{\mathrm{b}} \tag{9}$$

where

$$R_{\mathrm{b}} = \frac{\cos\theta}{\cos\theta_z} \tag{10}$$

$$\cos\theta = \sin\delta\sin\phi\cos\beta - \sin\delta\cos\phi\sin\beta\sin\gamma + \cos\delta\cos\phi\cos\beta\cos\omega$$

$$+ \cos\delta\sin\phi\sin\beta\cos\gamma\cos\omega + \cos\delta\sin\beta\sin\gamma\sin\omega \tag{11}$$

and

$$\cos\theta_z = \sin\delta\sin\phi + \cos\delta\cos\phi\cos\omega \tag{12}$$

T_{sky} was calculated as follows after Martin and Berdahl (1984):

$$T_{\mathrm{sky}} = T_{\mathrm{amb}}[\varepsilon_{\mathrm{o}} + (1 + \varepsilon_{\mathrm{o}})C]^{1/4} \tag{13}$$

where

$$\varepsilon_{\mathrm{o}} = 0.711 + 0.56\left(\frac{T_{\mathrm{dp}}}{100}\right) + 0.73\left(\frac{T_{\mathrm{dp}}}{100}\right)^2 + 0.13\cos\left[2\pi\frac{t}{24}\right] \tag{14}$$

and

$$C = n\varepsilon_{\mathrm{c}}\Gamma \tag{15}$$

where n is the fraction of the sky hemisphere covered by clouds, ε_{c} is the hemispherical cloud emissivity, and Γ a factor depending on the cloud base temperature.

Latent effects were incorporated in a steady-state moisture balance (Burch *et al.*, 1984; Cleary, 1985; Wilkes, 1989), written as

$$\sum_{\text{surface i}}^{S} A_{\mathrm{i}}\,\mathrm{Perm_i}\,P_{\mathrm{atm}}\left(\frac{w_{\mathrm{attic\,air}}}{0.622 + w_{\mathrm{attic\,air}}}\right) \div P_{\mathrm{o,l}} + \sum_{\text{surface i}}^{S} A_{\mathrm{i}} h_{w,\mathrm{i}}(w_{\mathrm{attic\,air}} - w_{w,\mathrm{i}})$$

$$+ Q_{\mathrm{air}}\rho_{\mathrm{air}}(w_{\mathrm{attic\,air}} - w_{\mathrm{o}}) = 0 \tag{16}$$

In Equation (16), the first term represents the rate of mositure transfer by diffusion through the attic components, the second term represents the moisture loss/gain by absorption/desorption of water vapour at wood surfaces, and the last term is the moisture transfer by exchange of attic air with the outdoor air. This expression was solved iteratively for $w_{\mathrm{attic\,air}}$. In Equation (16) the mass transfer coefficient, $h_{w,\mathrm{i}}$, was calculated using the Chilton–Colburn analogy between heat and

mass transfer (ASHRAE, 1989). The mass diffusivity term found in the Chilton–Colburn analogy was estimated using Sherwood's (1952) relation. The wood humidity ratio was estimated using a relation by Cleary (1985). Once the attic air humidity ratio, the mass transfer coefficient, and the wood humidity ratio had been calculated, the latent load was obtained using

$$q''_{\text{latent}} = h_{w,i}(w_{\text{attic air}} - w_{w,i})h_{fg} \tag{17}$$

where h_{fg} is the latent heat of vaporization of water.

EXPERIMENTATION AND MODEL VALIDATION

The model was validated by comparing its predictions to data obtained from monitoring two well-calibrated test houses. One house was used as a control house and the other as the experimental house. Both houses had almost-identical thermal performance. Ceiling heat flows and space cooling loads differed by less than 3 per cent. The experiments and the validations are presented in detail in Medina (1992). Only a brief description is provided here.

The experiments were carried out in Central Texas, where the climate is subtropical with hot summers and mild winters. The houses had normal dimensions of 13.38 m^2 (144 ft^2) with 17.8 cm (7 in) walls and had slab-on-grade foundations. The walls were constructed of a 5.08 cm (2 in) × 15.24 cm (6 in) (nominal) frame using paper-faced fibreglass batt insulation with a resistance level of 3.35 $m^2\,K\,W^{-1}$ (R-19). The exteriors and interiors were completed with 1.27 cm (0.5 in) sheathing and 1.27 cm (0.5) gypsum board, respectively. The ceiling was also made up of a 5.08 cm (2 in) × 15.24 cm (6 in) (nominal) framing and with 1.27 cm (0.5 in) gypsum board. Unfaced fibreglass insulation batts were used. An air infiltration retarder was placed in the interior part of the walls. The roof had asphalt shingles and 1.27 cm (0.5 in) plywood sheathing. The attic ventilation inlet area was located on the east side of each house and was a strip 3.81 cm (1.5 in) by 3.05 m (10 ft) long and 7.62 cm (3 in) above the ceiling frames. The outlet area was located 63.5 cm (25 in) above the ceiling frame on the west side of each house. The outlet was a 10.16 cm (4 in) diameter hole to which a fan, which induced airflow currents, was attached. Located at the exhaust side of each fan was a damper used to set the airflow rates.

Both houses were equipped with identical fan coil units (FCU), digital thermostats and water pumps. A chilled water circuit was constructed to supply both houses with a cold water/glycol solution (60/40) at approximately 4.4°C (40°F). Both houses were also equipped with identical electric resistance heaters rated at 1200 W (4100 Btu h^{-1}). These heaters were directly connected to the thermostats and to watt-hour counters and watt metres. The watt-hour counters tracked of the space heating load.

Each test house was instrumented with approximately 120 sensors. The sensors included type T thermocouples (T/C), surface heat flux meters (HFM), relative humidity transmitters (RH), water flow metres (WFM), watt-hour-metres (WHM), watt-metres (WM), and pressure sensors (PS). Besides the instrumentation from the houses, the ambient temperature, ground temperature, and global sun and sky radiation were measured at the test site. The data were collected at 1-min intervals and integrated hourly. Temperatures were recorded for the indoor room, attic air, roof, attic deck, and ceiling as well as across the fibreglass. Each test house was instrumented with five (5) HFMs with dimensions of 10.2 cm × 10.2 cm × 2.38 mm (4 in × 4 in × 3/32 in) with calibration traceable to the National Institute of Standards and Technology (NIST) standards. Four HFMs

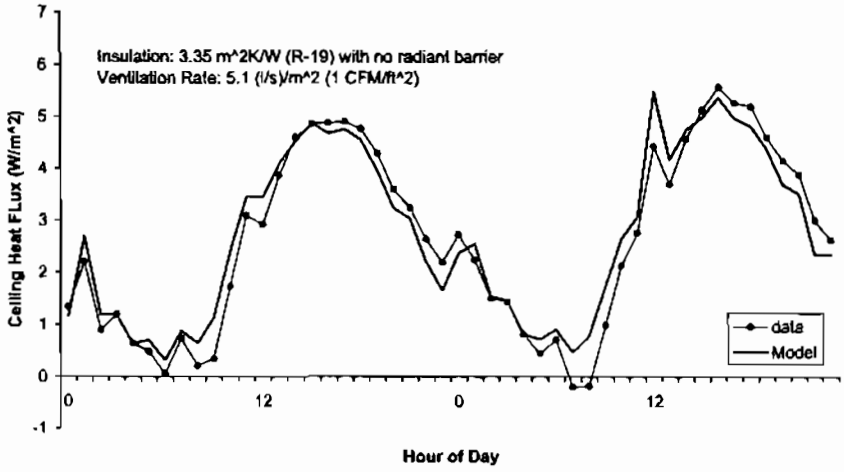

Figure 1. Model predictions versus experimental data (summer conditions, no radiant barrier).

were inside of each house and one in the floor of the attic. One of the four HFMs measured the flux through a ceiling joist. All reported heat flux readings were weighted averages of all HFMs. The total global sun and sky radiation on a horizontal surface was measured with a pyranometer with calibration traceable to NIST standards. An emissometer was used to measure the emissivity of any surface of interest. The pyranometer and emissometer were factory calibrated to within 3 and 1 per cent of full scale, respectively. Two RH sensors were located in each house, one indoors and one in the attic.

To assess the validity of the heat flux measurements, energy balances were obtained in which the energy blocked by the radiant barrier in the retrofit house was equivalent to the difference in space cooling loads between the houses. The indoor air temperatures of the houses were kept at $22.8 \pm 0.2°C$ during summers and at $20.9 \pm 0.2°C$ during winters. At any time during the experiments the indoor air temperature difference between the houses ($T_{\text{control house}} - T_{\text{retrofit house}}$) was never larger than 0.18°C.

The model was compared with the experimental data. The predictions were in good agreement with the data during both the peak and off-peak periods. Figure 1 depicts ceiling heat flux comparisons of the model predictions with experimental data. In this case, the data correspond to an attic under summer conditions, with no radiant barrier retrofit (no-RB case), with attic insulation level of $3.34\ m^2\,K\,W^{-1}$ (R-19), and with an attic ventilation rate of $5.1\ l\,s^{-1}\,m^{-2}$ of attic floor ($1\ CFM\ ft^{-2}$). For this case, the integrated per cent difference between model predictions and data was less than 2 per cent.

Figure 2 shows how the model predictions in the retrofit case compared to the data. In this case, the attic was under summer weather conditions and had a radiant barrier installed in the HRB configuration. The attic insulation level was $3.35\ m^2\,K\,W^{-1}$ (R-19) and the ventilation rate was $5.1\ l\,s^{-1}\,m^{-2}$ of floor area ($1\ CFM\ ft^{-2}$ of floor area). The integrated per cent difference was less than 4 per cent.

Figure 3 depicts comparisons under winter (and overcast) conditions. In this case, the attic had been retrofitted with a truss radiant barrier (TRB) and the attic was not vented. The attic insulation level was $3.35\ m^2\,K\,W^{-1}$ (R-19). The integrated percent difference between model predictions and data was also less than 4 per cent.

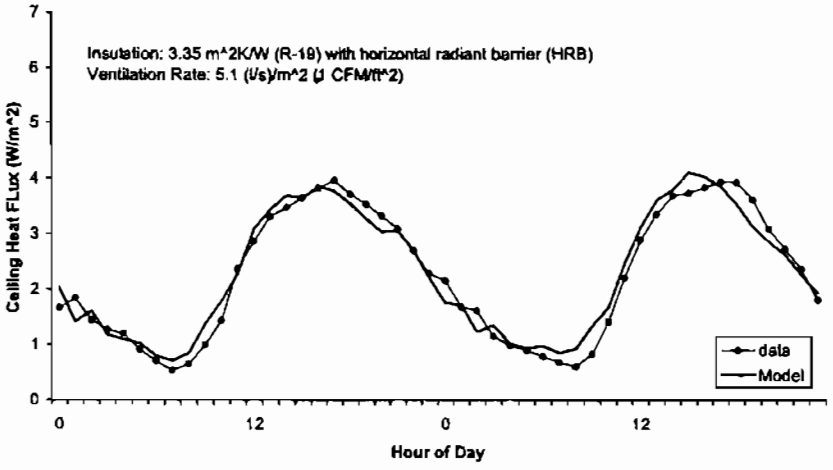

Figure 2. Model predictions versus experimental data (summer conditions, horizontal radiant barrier - HRB).

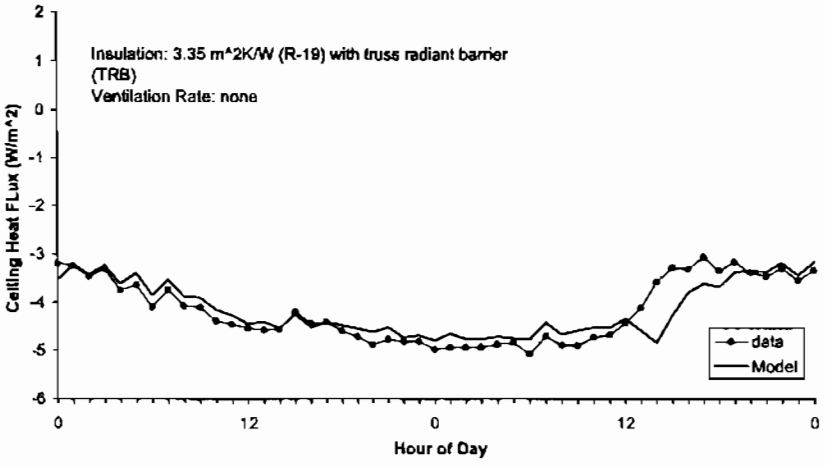

Figure 3. Model predictions versus experimental data (winter conditions, truss radiant barrier - TRB).

As presented, the model predicted reasonably well under the base case, the HRB case, and the TRB case during both cooling and heating seasons. The model predicted that under most cases, the HRB outperformed the TRB by few percentage points. This fact was confirmed during the experimental phase (Medina, 1992). Overall and under the conditions presented in this paper, a difference (model versus data) of less than 5 per cent was achieved. This degree of accuracy provided simulations with reliable estimates of heat flow reductions produced by the radiant barriers for hourly and seasonal simulations.

RESULTS AND DISCUSSION

Roof absorptivity effects on the performance of radiant barriers

The fraction of the incident solar energy absorbed by the roof of a residence significantly affects the overall heat gain or loss to or from the conditioned space, particularly in places were the amount of solar radiation is abundant. Data on solar absorptivity of roofing materials is limited. In this study, a test was conducted in which the temperatures of two materials of known solar absorptivity were compared to the temperature of the shingles of the houses being modelled. By comparing and equating the Sol-air temperatures, the absorptivity value of the shingles was approximated. This value was 0.78. Several values of shingle absorptivity below 0.78 were simulated. The results are presented in Figure 4.

The results suggest that during the cooling season the performance of both the HRB and the TRB improved slightly, at about the same rate, as the roof absorptivity increased. When the amount of the solar energy absorbed by the roofing material increased, the attic deck temperatures increased and the radiation from the deck to the top-of-the-fibreglass became more dominant. This rate of heat transfer in the control attic increased at a faster rate than it did in either of the HRB and TRB cases, thus increasing the seasonal percent reductions produced by the radiant barriers. During the heating season, a decrease in SCHFR was observed. The explanation was the same. Increasing the roof absorptivity produced a cumulative heat loss from the conditioned space that became lower in the no-RB than in either the HRB or TRB cases and led to a decrease in the SCHFR. The drop in radiant barrier performance during this season was substantial. However, absorptivity of roofing materials is seldom larger than 0.80. Over typical roofing absorptivity range, the performance of the radiant barriers was basically unchanged.

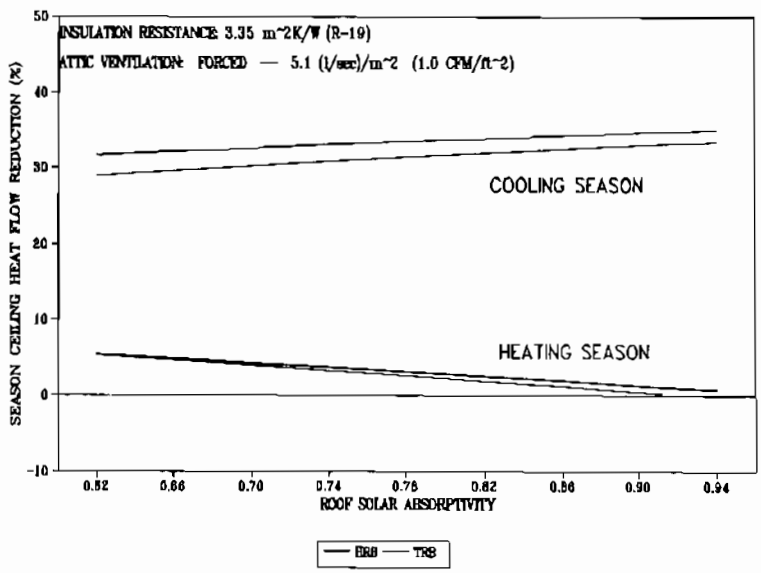

Figure 4. Radiant barrier performance as a function of roof absorptivity (insulation resistance: 3.35 $m^2 K W^{-1}$, R-19, with attic airflow rate: 5.1 $l s^{-1} m^{-2}$, 1.0 CFM ft^{-2}).

Radiant barrier emissivity effects on the performance of radiant barriers

The emissivity of the radiant barrier blocks most of the infrared radiation from the attic deck to the top-of-the-fibreglass. Aluminium is used because of its low emissivity. The emissivity of radiant barriers changes because of dust and contaminant accumulation on its surface, especially for the case of the HRB. Dust accumulates because it travels with the attic ventilation air. Dust size and quantity accumulated depend on the ventilation flowrate, type of flow arrangement, and location of the building.

Several references have dealt with dust accumulation and its effect on the emissivity of radiant barriers (Hall, 1988; Yarbrough *et al.*, 1989; Noboa, 1991) and all predicted that dust increased the emissivity value of the barriers. In this study, the ceiling load reduction was plotted against different RB emissivity values. This is shown in Figure 5.

Cooling season results indicated that the performance of the radiant barriers dropped substantially as the emissivity increased. In the case of the HRB, the performance dropped at an average rate of 14.7 percentage points per 0.1 unit of emissivity increment. This rate also dropped from 16/0.1 to 5.2/0.1 as the emissivity increased. In the case of the TRB, the seasonal reductions dropped at a slightly lower rate, 6.4 percentage points per 0.1 units of emissivity increment. This rate also decreased from 9.4/0.1 to 5/0.1 as the emissivity increased. An overlap in both curves was observed at an emissivity of 0.15. From this point on, the TRB seemed more effective than the HRB. One possible explanation set forth was the extra air space that was formed between the barrier and the attic deck. This space represented a significant resistance to heat flow from the deck to the top-of-the-fibreglass. Heating season results suggested an improvement in the performance of the radiant barriers. At higher values of emissivity, the net cumulative amount of heat loss from the conditioned space was lower because more heat was admitted into

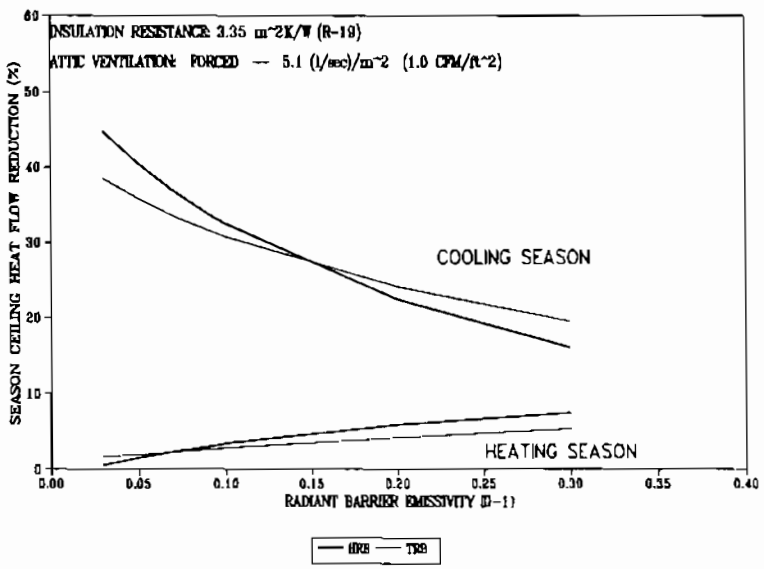

Figure 5. Radiant barrier performance as a function of radiant barrier emissivity (insulation resistance: 3.35 $m^2 K W^{-1}$, R-19, with attic airflow rate: 5.1 $l s^{-1} m^{-2}$, 1.0 CFM ft^{-2}).

the conditioned space from the attic during sunny periods. Also, the HRB seemed to outperform the TRB because more heat was lost from the attics through the end-gables in the TRB attic. In essence, radiant barrier emissivity proved to be the parameter that affected its performance the most.

Attic ventilation flowrate effects on the performance of radiant barriers

The purpose of attic ventilation is to remove heat from the attic during the cooling season and to reduce moisture build-up during the heating season. A ventilated attic produces lower ceiling heat fluxes into the conditioned space than a non-vented attic. The amount of ventilation required to reduce the temperature of the attic is small. Experimental results have shown that attic ventilation has little effect on the performance of radiant barrier once a small threshold ventilation of approximately $1.3\,l\,s^{-1}\,m^{-2}$ ($0.25\,CFM\,ft^{-2}$) has been reached (Medina *et al.* 1992). The model confirmed the experimental results. Attic airflow ranges were extended to rates that were not achieved by experimental means. The results are presented in Figure 6.

For the cooling season, and in the case of the HRB, the data showed that the differences in ceiling heat flux reductions were more detectable before the airflow rate reached $1.3\,l\,s^{-1}\,m^{-2}$ of attic floor ($0.25\,CFM\,ft^{-2}$). Once the attic airflow surpassed this rate, the per cent reductions in ceiling heat flux remained constant regardless of airflow rate just as the earlier experiments had suggested (Medina *et al.*, 1992). Before the attic ventilation rate reached $1.3\,l\,s^{-1}\,m^{-2}$ ($0.25\,CFM\,ft^{-2}$), the results implied an increase in percent heat flow reductions from approximately 28 per cent to approximately 33 per cent; 28 per cent being the per cent reduction in a non-vented attic. At a ventilation rate of $0\,l\,s^{-1}\,m^{-2}$, the model predicted that the difference in top-of-the-fibreglass temperature difference between the control and retrofit attics was the

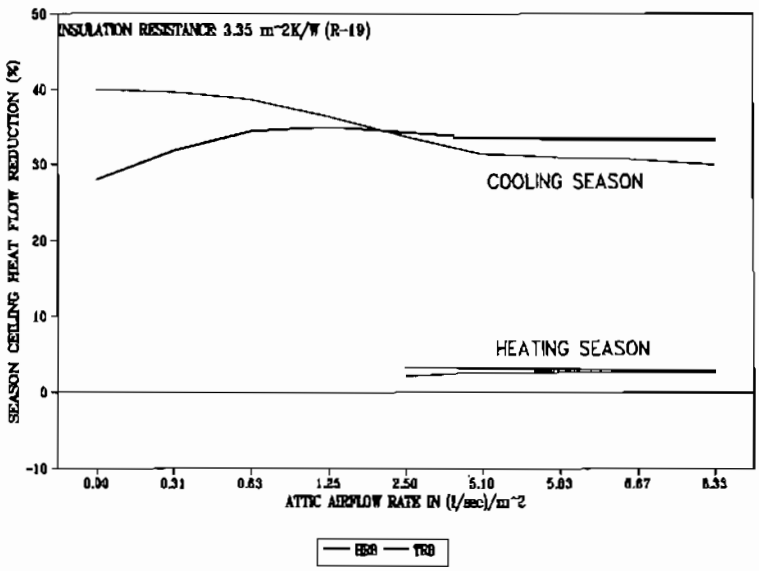

Figure 6. Radiant barrier performance as a function of attic airflow rate (insulation resistance: $3.35\,m^2\,K\,W^{-1}$, R-19).

smallest it could be, yielding a relatively lower ceiling heat flow reductions. At this point, the model predicted the hottest possible (averaged over the season) fibreglass surface temperatures. As air entered the attic, these temperatures cooled down. The top-of-fibreglass temperatures cooled down faster in the HRB case and remained at approximately the same temperature while the temperature of the fibreglass in the no-RB case worked its way down at a slower rate as a function of attic airflow rate, thus yielding larger and growing temperature differences between these top-of-the-fibreglass temperatures in the control and retrofit cases. This is why the curve appears in an increasing trend up until an attic flowrate of $1.3\,l\,s^{-1}\,m^{-2}$ ($0.25\,CFM\,ft^{-2}$) was reached. The TRB exhibited a different trend. The seasonal ceiling heat flow reductions showed a continual decrease from $0\,l\,s^{-1}\,m^{-2}$, except that it levelled off at approximately $5.1\,l\,s^{-1}\,m^{-2}$ ($1\,CFM\,ft^{-2}$). At $0\,l\,s^{-1}\,m^{-2}$, the difference in cumulative heat flows between the retrofit and non-retrofit attics was at its maximum value. One possible explanation is that the radiation blockage produced by the TRB substantially reduced the top-of-the-fibreglass temperature in the retrofit case when compared to the control case. This difference in cumulative heat flows and of fibreglass temperatures decreased once air entered the attics. In an attic retrofit with a TRB, this fibreglass temperature was essentially that of the ambient air. These results suggested that the top-of-the-fibreglass temperature in the TRB case was substantially lower than in the HRB case up until an attic airflow rate of approximately $1.9\,l\,s^{-1}\,m^{-2}$. At low flowrates, the TRB should be more effective than the HRB because an extra air space of at least 8.9 cm (3.5 in) is formed. The air that circulated through the attic was what made the HRB a more effective combination. During the heating season the model could not be extended to ranges of airflow lower than $2.5\,l\,s^{-1}\,m^{-2}$ because, under Austin whether and at low flowrates, the model did not converge. However, for airflows larger than $2.5\,l\,s^{-1}\,m^{-2}$ the model suggested no major changes in the reductions produced by the radiant barriers. Under both configurations it was observed that the SCHFR leveled off after a certain flowrate had been reached for both cooling and heating season. One explanation to this phenomenon is that, above a certain flowrate, the convective component no longer had a major effect in the overall heat transfer.

Roof slope effects on the performance of radiant barriers

Residences are built with attics of different shapes and forms. It was thought that roof slope could be a parameter that would influence the amount of ceiling heat gain in and out of the residence. The model was used to simulate different roof slopes to predict the per cent reductions produced by the radiant barriers. The results are shown in Figure 7.

No significant changes were observed in the amount of ceiling load gained or lost by the attic with the HRB configuration. The results suggested that the attic shape above the radiant barrier was immaterial. In the case of the TRB configuration the changes were more noticeable, as was expected. As the roof slope increased, the ceiling heat gained in the TRB ceiling increased, lowering the overall seasonal per cent reductions in the summer and increasing them in the winter. The reason is that the gable ends played a more important role because as the attics became steeper the area of the gable ends increased. Radiant barriers did not cover the gable ends. Covering the end gables with radiant barriers could also prove to be a problem in some house orientations. The simulated houses faced south and the gable ends faced east and west. In some situations, a covered gable end would trap heat within the attic instead of letting this heat escape because most attic air temperatures are higher than outdoor temperatures.

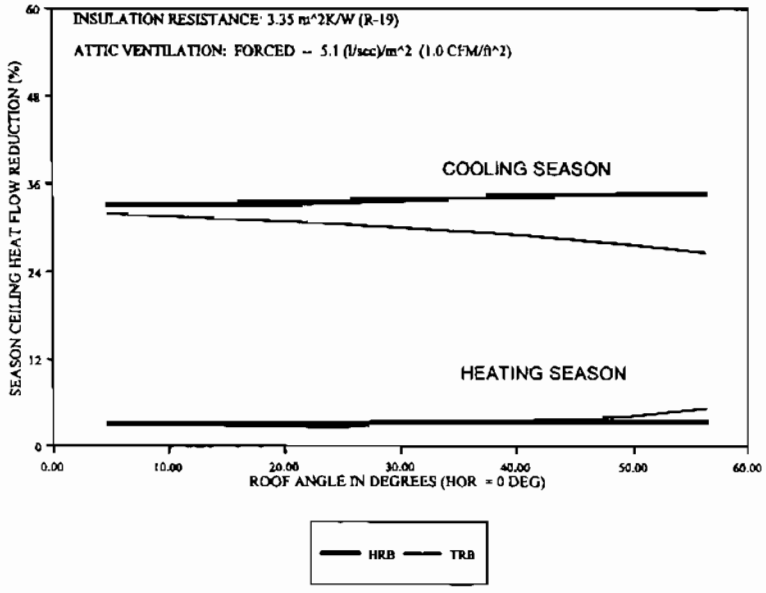

Figure 7. Radiant barrier performance as a function of roof angle (insulation resistance: 3.35 $m^2 K W^{-1}$, R-19, with attic airflow rate: 5.1 $l s^{-1} m^{-2}$, 1.0 CFM ft^{-2}).

CONCLUSIONS

A heat balance model was developed to investigate the effects that some parameters would have on the performance of radiant barriers. The model was validated against experimental data and was found to predict with good accuracy. Parametric analyses were conducted to assess the performance of the radiant barriers as a function of shingle absorptivity, radiant barrier emissivity, attic ventilation flowrate, and roof slope. It was found that only the emissivity of the radiant barriers had first order effects on their performance. Variations in the performance of the HRB were minimal in the other three. The TRB showed more variations because of the uncovered end-gables.

Increases in RB emissivity significantly decreased the RB seasonal ceiling heat flow reductions during the cooling season for both the HRB and TRB. A reduction of over 50 per cent in SCHFR was estimated when the emissivity increased from 0.03 to 0.3. During the heating season, the opposite was observed because at higher values of emissivity more heat was allowed into the conditioned space thus decreasing the net losses.

Changes in shingle absorptivity values produced slight changes in RB performance. Over typical values of roofing absorptivities, the performance of the radiant barriers was basically unchanged. Similarly, for vented attics, once an attic airflow rate of 1.3 $l s^{-1} m^{-2}$ of attic floor had been reached, the HRB configuration had no noticeable changes in performance. For the TRB the same was true after an airflow rate of 5.1 $l s^{-1} m^{-2}$ of attic floor. The reason was found in the top-of-the-fibreglass temperatures at different attic airflow rates. For the HRB configuration, convection effects were not as significant past 1.3 $l s^{-1} m^{-2}$ of attic floor. In general, the TRB produced lower attic temperatures than the HRB for airflow rates less than 1.9 $l s^{-1} m^{-2}$ of attic floor.

No significant changes were observed in the amount of ceiling load gained or lost by the attic with the HRB configuration as a function of roof slope. The results suggested that the attic shape above the radiant barrier had no impact on its performance. In the case of the TRB configuration the changes were more noticeable because the gable ends played a more important role since, as the attics became steeper, the area of the gable ends increased and the radiant barriers did not cover the gable ends.

ACKNOWLEDGEMENTS

The author acknowledges the support of Dr W. Dan Turner and the staff of the Energy Systems Laboratory. This work was funded by the State of Texas Energy Research and Applications Program and the University of Kansas.

APPENDIX: NOMENCLATURE

A	= surface area
CR	= common ratio
G	= radiation coefficient
h, hi, ho	= heat transfer coefficient
h_{fg}	= latent heat of vaporization
hri, hro	= radiation heat transfer coefficients
HRB	= horizontal radiant barrier
I	= irradiation
k	= thermal conductivity
L	= length, characteristic length
n	= cloud cover fraction, index
Nu	= Nusselt number
P	= pressure
Perm	= permeability
Q	= heat flow, volumetric flowrate
q''	= heat flux
T	= temperature
Tr	= reference temperature
TRB	= truss radiant barrier
Tsi	= inside surface temperature
Tso	= outside surface temperature
w	= humidity ratio
X, Y, Z	= conduction transfer functions
β	= tilt angle
χ	= radiation matrix
δ	= kroneker delta, declination angle
Δ	= time increment
ε	= thermal emissivity
ϕ	= angle, latitude, relative humidity
Γ	= cloud emissivity factor
γ	= surface azimuth angle
θ	= incidence angle
σ	= Stefan–Boltzman constant
ω	= hour angle
ψ	= inverse of matrix

Subscripts

0, 1, 2, ...	= time denoting index (conduction transfer functions)
amb	= ambient conditions
b	= beam
cond	= condensation
d	= diffuse
dp	= dew point
F	= forced
i	= denotes surface, index, indoor conditions
j	= denotes time, index
k	= denotes surface
N	= natural
$n\Delta$	= time step
o	= outdoor conditions
rad	= radiative
x	= local

Index

N	= number of surfaces
S	= number of time steps

REFERENCES

ASHRAE. 1989. *Handbook of Fundamentals*. American Society of Heating, Refrigeration, and Air Conditioning Engineers: Atlanta, GA.

ASHRAE. 1997. *Handbook of Fundamentals*. American Society of Heating, Refrigeration, and Air Conditioning Engineers: Atlanta, GA.

Burch DM, Lemay MR, Rian BJ, Parker EJ. 1984. Experimental validation of an attic condensation model. *ASHRAE Transactions*, Part 2A **20**:59–77.

Chen TS, Armaly BF, Ramachandran N. 1986. Correlations for laminar mixed convection flows on vertical, inclined, and horizontal flat plates. *Journal of Heat Transfer* **108**:835–840.

Churchill SW. 1977. A comprehensive correlating equation for laminar assisting, forced and free convection. *A.I.Ch.E. Journal* **23**:10–16.

Cleary PG. 1985. Moisture control by attic ventilation -an in-situ study. *ASHRAE Transactions*, Part 1, **91**:227–239.

Energy Information Administration/*Monthly Energy Review*. 1998. U.S. Department of Energy: Washington DC.

Hall JA. 1988. Radiant barrier testing to assess the effects of dust accumulation, attic ventilation, and other key variables. *TVA Report No.TVA/OP/EDT-88/25*, Tennessee Valley Authority, Office of Power, Division of Energy Demonstration and Technology.

Martin A, Berdahl. 1984. Characteristics of infrared sky radiation in the United States. *Solar Energy* **33**:321–336.

Medina MA. 1992. Development of a transient heat and mass transfer model of residential attics to predict energy savings produced by the use of radiant barriers. *Ph.D. Dissertation*, Department of Mechanical Engineering, Texas A&M University, College Station, TX.

Medina MA, O'Neal DL, Turner WD. 1992. Effect of attic ventilation on the performance of radiant barriers. *ASME Journal of Solar Energy Engineering* **114**:234–239.

Medina MA, O'Neal DL, Turner WD. 1998a. A transient heat and mass transfer model of residential attics used to simulate radiant barrier retrofits, Part I: development. *ASME Journal of Solar Energy Engineering* **120**:32–38.

Medina MA, O'Neal DL, Turner WD. 1998b. A transient heat and mass transfer model of residential attics used to simulate radiant barrier retrofits, Part II: validation and simulations. *ASME Journal of Solar Energy Engineering* **120**:39–44.

Noboa HL. 1991. Influence of dust on the emissivity of radiant barriers. *Masters Thesis*, Department of Mechanical Engineering, Texas A&M University, College Station, TX.

Pedersen CO, Fisher DE, Spitler JD, Liesen RJ. 1998. *Load Calculation Principles—Advance Copy*. American Society of Heating, Refrigerating, and Air-Conditioning Engineers: Atlanta, GA.

Sherwood TK, Pigford RL. 1952. *Absorption and Extraction*. McGraw-Hill: New York.

Wilkes KE. 1989. Modeling of residential attics with radiant barriers. *Proceedings of the Fifth Annual Symposium on Improving Building Energy Efficiency in Hot and Humid Climates*, Houston, TX; 161–168.

Yarbrough D, Cook J, Wilkes K. 1989. Contamination of reflective foils in horizontal applications and its effects on thermal performance. *ASHRAE Conference*, Vancouver, BC, Canada.